Contents

The following Communications have been judged by at least two referees to be "very important papers" and will be published online at www.angewandte.org soon:

S. Ghosh, A. Mukherjee, P. J. Sadler, S. Verma**
Periodic Iron Nanomineralization in Human Serum Transferrin Fibrils

M. Murata, Y. Ochi, F. Tanabe, K. Komatsu, Y. Murata**
Internal Magnetic Fields of Dianions of Fullerene and Its Cage-Opened Derivatives Studied with Encapsulated H_2 as an NMR Spectroscopic Probe

S. A. Joyce, A. O. Brachmann, I. Glazer, L. Lango, G. Schwär, D. J. Clarke, H. B. Bode**
Bacterial Biosynthesis of a Multipotent Stilbene

*M. Schulz-Dobrick, M. Jansen**
Intercluster Compounds Consisting of Gold Clusters and Fullerides: $[Au_7(PPh_3)_7]C_{60}\cdot$THF and $[Au_8(PPh_3)_8](C_{60})_2$

*Y. Bolshan, R. A. Batey**
Enamide Synthesis by Copper-Catalyzed Cross-Coupling of Amides and Potassium Alkenyltrifluoroborate Salts

*J. S. Lim, Y. S. Lee, S. K. Kim**
Control of Intramolecular Orbital Alignment in the Photodissociation of Thiophenol: Conformational Manipulation by Chemical Substitution

News

Books

Highlights

Enzyme Models

Cleaning up without enzymes: Alkyl mercury cations are poorly degradable. Protonolysis of Hg–C bonds by bacteria takes place with the aid of organomercury lyase, and functional models based on dihydroimidazolethione ligands have been recently reported. Relatively high metal coordination numbers (e.g. 4, see figure) are the key to bond activation and thus to non-enzymatic detoxification of the neurotoxic methylmercury cation.

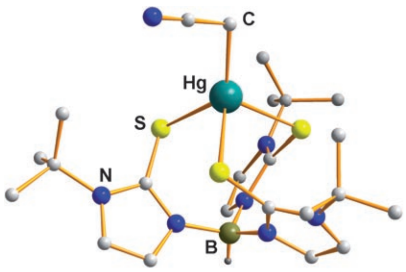

P_4 Activation

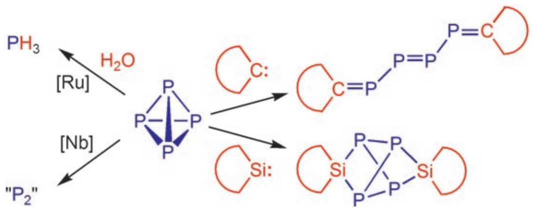

Unlocking the cage: New methods for the activation of white phosphorus have demonstrated that transition-metal complexes may facilitate some remarkable new transformations of P_4. Furthermore, main-group species such as carbenes and silylenes may also promote the formation of synthetically important phosphorus-rich compounds.

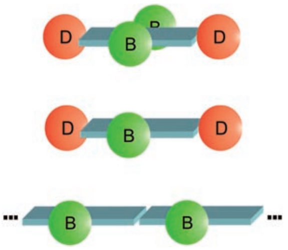

Lateral thinking: Molecular solids with tunable color and excellent emission efficiencies or increased electron affinities have been obtained by lateral boryl substitution on a π-delocalized framework (see picture, D = donor group, B = boryl group). This approach gives rise to a new design principle for organic optoelectronic materials.

Reviews

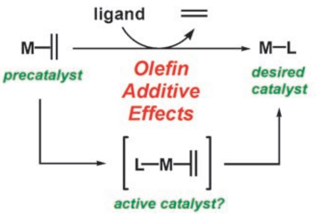

Olé to olefins: Olefins as components of transition-metal-catalyzed reactions can influence the outcome of a reaction through increased activity, stability, or selectivity. This Review outlines the interaction of olefins with transition metals and documents examples of olefins that influence catalytic reactions; a particular focus is on cross-coupling reactions.

Communications

Starting gate: A molecular logic gate is based on chemosensors that change their fluorescence intensity in response to various inputs (pH, metal ions) in a microfluidic system. A combinatorial circuit, such as a half adder (see picture), uses fluorescein (green) and rhodamine B (red) derivatives that respond to pH. A logic gate with a protein and Cu^{2+} ions as inputs is also described.

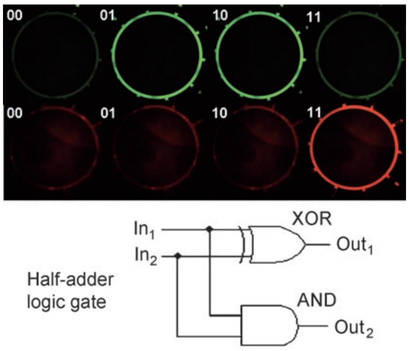

For the USA and Canada: ANGEWANDTE CHEMIE International Edition (ISSN 1433-7851) is published weekly by Wiley-VCH, PO Box 191161, 69451 Weinheim, Germany. Air freight and mailing in the USA by Publications Expediting Inc., 200 Meacham Ave., Elmont, NY 11003. Periodicals postage paid at Jamaica, NY 11431. US POSTMASTER: send address changes to *Angewandte Chemie*, Wiley-VCH, 111 River Street, Hoboken, NJ 07030. Annual subscription price for institutions: US$ 7225/6568 (valid for print and electronic / print or electronic delivery); for individuals who are personal members of a national chemical society prices are available on request. Postage and handling charges included. All prices are subject to local VAT/sales tax.

Molecular Sensors

C. He, Z. Lin, Z. He, C. Duan,* C. Xu, Z. Wang, C. Yan* ______ **877 – 881**

Metal-Tunable Nanocages as Artificial Chemosensors

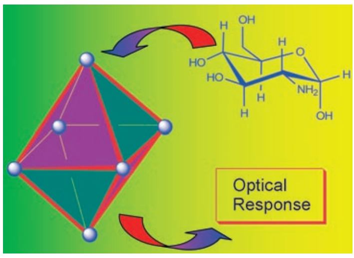

Molecular design: Metal-tunable octahedral nanocages that act as molecular chemosensors are generated by a new strategy (the metals can be transition metals or lanthanides). Amide groups in the supramolecular structures act as guest-accessible functional sites. These interact with glucosamine molecules and function as efficient communicators to convert the recognition information into metal-tunable chromogenic and fluorogenic responses (see picture).

Hydrogen-Storage Materials

J. Yang,* A. Sudik, D. J. Siegel, D. Halliday, A. Drews R. O. Carter III, C. Wolverton, G. J. Lewis, J. W. A. Sachtler, J. J. Low, S. A. Faheem, D. A. Lesch, V. Ozolinš ______ **882 – 887**

A Self-Catalyzing Hydrogen-Storage Material

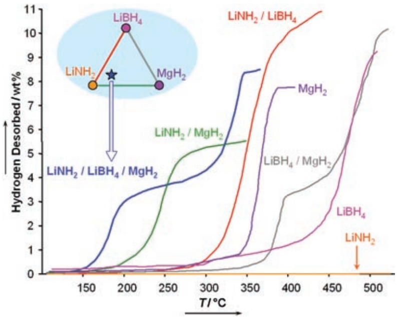

Greater than the sum of its parts: Hydrogen storage in complex hydrides is accelerated by using the ternary composite 2 $LiNH_2/LiBH_4/MgH_2$, which exhibits a "self-catalyzing" reaction pathway that results in faster H_2 desorption, lower desorption temperatures, and suppression of NH_3 release in comparison to the constituent binary composites (see diagram). The enhanced properties arise from the incorporation of an ionic liquid phase ($Li_4BH_3H_{10}$) and from ancillary-reaction seeding of a reversible H_2 storage reaction.

Indole Synthesis

T. Jensen, H. Pedersen, B. Bang-Andersen, R. Madsen, M. Jørgensen* ______ **888 – 890**

Palladium-Catalyzed Aryl Amination–Heck Cyclization Cascade: A One-Flask Approach to 3-Substituted Indoles

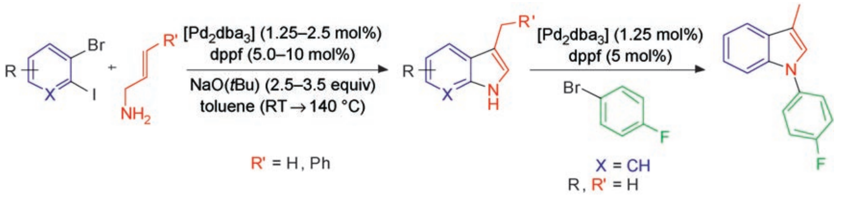

Two for the price of one: A Pd/dppf-based catalyst provides access to the title compounds from 1,2-dihalogenated aromatic compounds and allylic amines in a single reaction flask. The initial aryl amination step occurs with excellent selectivity for the aryl iodide to ensure the formation of a single indole regioisomer, which can be functionalized in situ by N-arylation (see scheme). dba = dibenzylideneacetone, dppf = 1,1′-bis(diphenylphospanyl)ferrocene.

Organolithium Chemistry

C. Fressigné,* A.-L. Girard, M. Durandetti, J. Maddaluno* ______ **891 – 893**

Intramolecular Carbolithiation of Alkynes: *anti* Selectivity

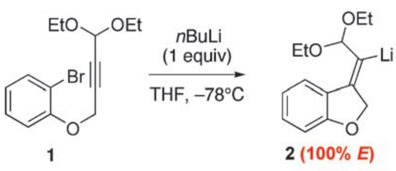

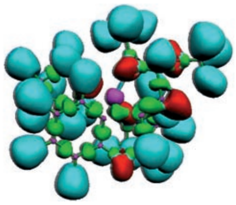

A stereochemical twist in the tale: The treatment of the propargylic acetal **1** with one equivalent of *n*-butyllithium provided the dihydrobenzofuran **2** with an exocyclic *E* double bond. The results of DFT calculations suggest that strong coordination between the lithium cation and one oxygen atom of the acetal group drives the triple bond toward an *E* alkene. (A representation of the electron distribution near the transition state is shown on the right.)

Self-Assembled Ligands

S. A. Moteki, J. M. Takacs* ___ 894 – 897

Exploiting Self-Assembly for Ligand-Scaffold Optimization: Substrate-Tailored Ligands for Efficient Catalytic Asymmetric Hydroboration

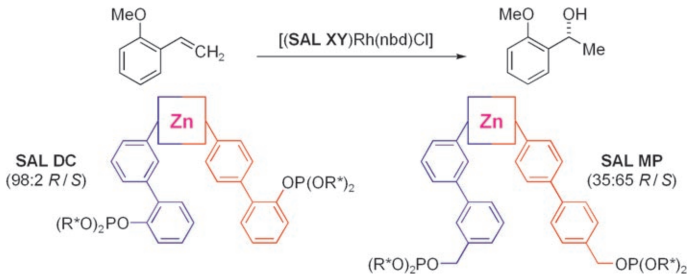

Mix and match: A self-assembled ligand library (**SAL XY**) affords a wide range of *R*/*S* ratios in Rh-catalyzed asymmetric hydroboration (see scheme; nbd = 2,5-norbornadiene, R* is a chiral substituent). Ligand-scaffold optimization reveals "substrate-tailored" ligands that afford high regio- and enantioselectivity for a variety of *ortho*-substituted styrene derivatives.

Enzyme Probes

E. C. Glazer, Y. H. L. Nguyen, H. B. Gray, D. B. Goodin* ___ 898 – 901

Probing Inducible Nitric Oxide Synthase with a Pterin–Ruthenium(II) Sensitizer Wire

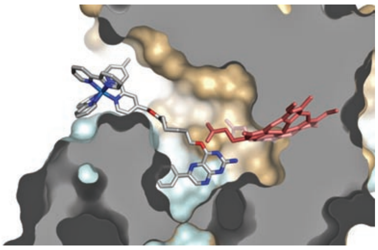

Binding by the light: A photoactive ruthenium(II)–pterin wire designed to target the tetrahydrobiopterin (H_4B) binding site of inducible nitric oxide synthase ($iNOS_{heme}$) binds to $iNOS_{heme}$ in a competitive fashion with the natural cofactor and other small molecules; thus it can be used to screen potential inhibitors. Rapid charge injection to the heme occurs upon 450-nm excitation of an $iNOS_{heme}$/wire conjugate.

Foam Films

W. Bu, J. Jin, I. Ichinose* ___ 902 – 905

Foam Films Obtained with Ionic Liquid

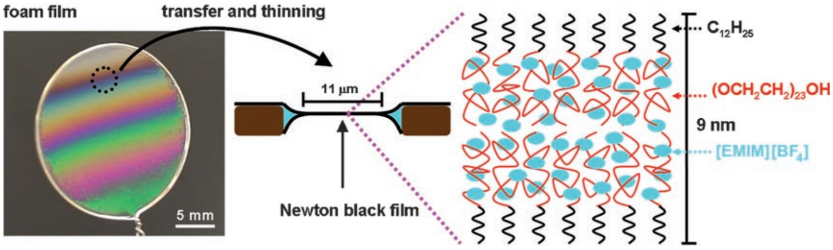

Film noir: A centimeter-scale foam film of nonionic surfactant can be prepared by using the ionic liquid 1-ethyl-3-methylimidazolium tetrafluoroborate ($[EMIM][BF_4]$). On transferring to a substrate with submillimeter holes, the black films on the holes spontaneously become thinner to give reversed bilayers solvated with the ionic liquid (see picture). They are stable under ultrahigh vacuum conditions and at temperatures higher than 150 °C.

Multicolor Tuning

F. Wang, X. Xue, X. Liu* ___ 906 – 909

Multicolor Tuning of (Ln, P)-Doped YVO_4 Nanoparticles by Single-Wavelength Excitation

Chemical chameleon: Two complementary approaches to emission color modulation are based on (Ln, P)-doped YVO_4 nanoparticle systems. The emission wavelengths and intensity ratios can be controlled using different host–activator systems and dopant concentrations. This approach allows access to a wide range of colors (see picture) using single-wavelength excitation.

Contents

Domino Reactions

G. Bojase, A. D. Payne, A. C. Willis,
M. S. Sherburn* ______ **910 – 912**

One-Step Synthesis and Exploratory Chemistry of [5]Dendralene

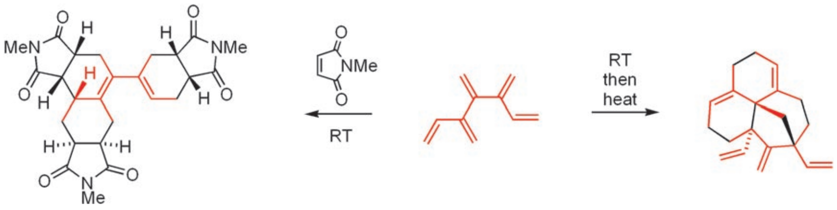

Complex polycycles made simple: A practical synthesis of the simplest cross-conjugated pentaene, [5]dendralene, is reported. The hydrocarbon undergoes controllable and atom-efficient domino sequences (see scheme) to generate complex polycyclic frameworks in an operationally simple manner.

Chiral Sensors

P. Kurzawski, A. Bogdanski, V. Schurig,
R. Wimmer, A. Hierlemann* ___ **913 – 916**

Opposite Signs of Capacitive Microsensor Signals upon Exposure to the Enantiomers of Methyl Propionate Compounds

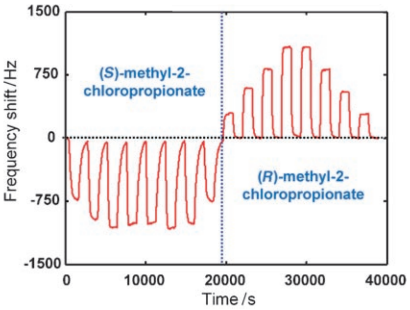

Capacitive chemical sensors, coated with modified cyclodextrins, provide antipode signals upon exposure to the enantiomers of methyl propionate compounds, thus allowing an unambiguous determination of the enantiomer identity (see graphic). The dielectric coefficients of the enantiomer–receptor complexes significantly differ, so that this simple sensor technique can be used to detect the subtle effects of different molecular orientations.

Oscillating Microgels

D. Suzuki, T. Sakai,
R. Yoshida* ______ **917 – 920**

Self-Flocculating/Self-Dispersing Oscillation of Microgels

Self-oscillating microgels have been obtained by introducing a Ru catalyst for the Belousov–Zhabotinsky (BZ) reaction into a cross-linked copolymer. In this microgel system, the chemical energy of the BZ reaction is converted to rhythmic swelling/deswelling with self-flocculating/self-dispersing oscillation of the microgel around its phase-transition temperature (see scheme; Ru(bpy)$_3$ denotes a Ru tris-bipyridine complex bearing a vinyl group).

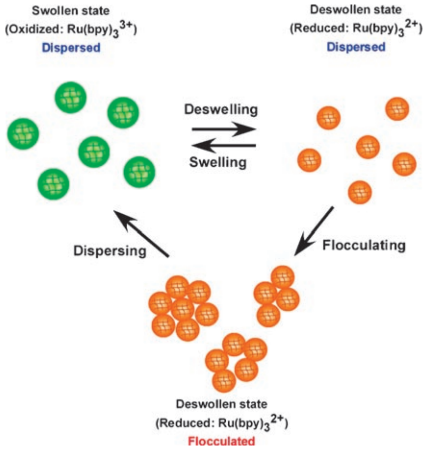

Membrane Transport

A. Perez-Velasco, V. Gorteau,
S. Matile* ______ **921 – 923**

Rigid Oligoperylenediimide Rods: Anion–π Slides with Photosynthetic Activity

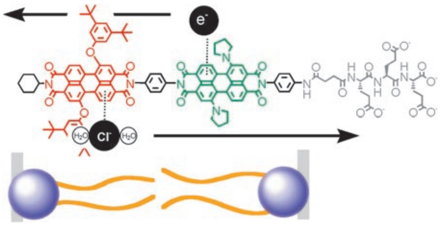

Slide rules: A new class of membrane-active rigid-rod molecules comprising π-acidic, n-semiconducting oligoperylenediimides is introduced (see picture). They are able to combine passive anion transport across lipid bilayers with photoactive electron transport in the other direction across intact vesicle membranes. Thus, the compounds demonstrate artificial photosynthetic activity.

Metal Macrocycles

L. P. Engelhardt, C. A. Muryn,
R. G. Pritchard, G. A. Timco,* F. Tuna,
R. E. P. Winpenny* ______ **924–927**

Octa-, Deca-, Trideca-, and Tetradecanuclear Heterometallic Cyclic Chromium–Copper Cages

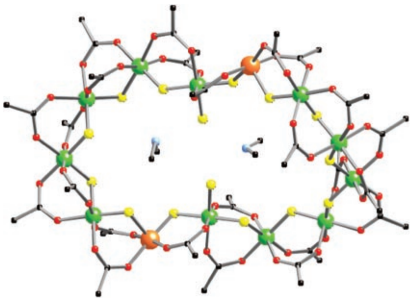

Ring around the amine: Reactions which give heterometallic Cr_xCu_y rings can be controlled through choice of reaction times, and the mixed products can be separated and crystallized. These new compounds include Cr_7Cu, Cr_8Cu_2, $Cr_{12}Cu_2$, and $Cr_{11}Cu_2$ rings (see structure; Cu orange, Cr green, F yellow, O red, N blue, C black). The last compound is the largest ring known with an odd number of metal atoms.

Organoboron Compounds

Y. Yamamoto,* M. Takizawa, X.-Q. Yu,
N. Miyaura* ______ **928–931**

Cyclic Triolborates: Air- and Water-Stable Ate Complexes of Organoboronic Acids

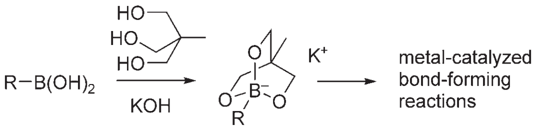

A borate in the hand is a convenient reagent for palladium- and copper-catalyzed C–C and C–N bond-forming reactions, especially when, like the title bench-stable complexes, it demonstrates high transmetalation efficiency. Cyclic triolborates can be synthesized readily from organoboronic acids (see scheme), can be handled and stored without special precautions, and are relatively soluble in organic solvents.

Asymmetric Catalysis

S.-F. Zhu, C. Chen, Y. Cai,
Q.-L. Zhou* ______ **932–934**

Catalytic Asymmetric Reaction with Water: Enantioselective Synthesis of α-Hydroxyesters by a Copper–Carbenoid O–H Insertion Reaction

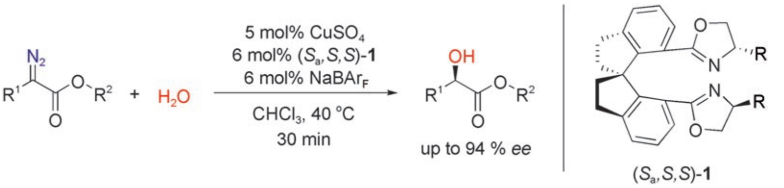

(S_a,S,S)-**1**

Taking on water: A novel catalytic asymmetric metal–carbenoid insertion reaction with water has been developed with copper complexes of chiral spiro bisoxazoline ligands as catalysts. This reaction provides an efficient and practical procedure for preparing chiral α-hydroxyesters and acids starting from readily available materials in high yields and enantioselectivities. $BAr_F^- = [B\{3,5\text{-}(CF_3)_2C_6H_3)\}_4]^-$.

Cascade Reactions

M. B. Runge, M. T. Mwangi, A. L. Miller II,
M. Perring, N. B. Bowden* ______ **935–939**

Cascade Reactions Using $LiAlH_4$ and Grignard Reagents in the Presence of Water

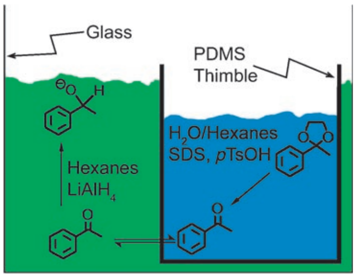

Divided we stand, together we fall: Incompatible reagents, such as water and $LiAlH_4$, Grignard, or cuprate reagents, can be site-isolated on either side of a polydimethylsiloxane (PDMS) thimble (see scheme; SDS = sodium docecyl sulfate) for cascade reactions. The hydrophobic nature of the PDMS membrane prohibits polar molecules, such as water, from diffusing across the membrane.

Contents

Fe-Catalyzed Hydrogenation

C. Sui-Seng, F. Freutel, A. J. Lough,
R. H. Morris* ———— **940 – 943**

Highly Efficient Catalyst Systems Using Iron Complexes with a Tetradentate PNNP Ligand for the Asymmetric Hydrogenation of Polar Bonds

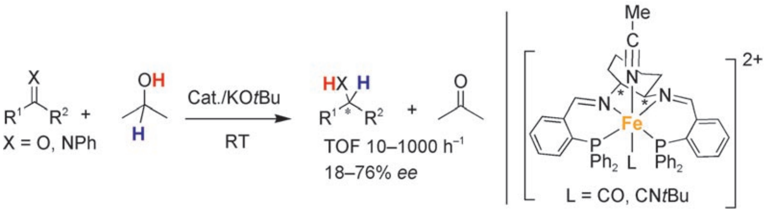

Iron competes with pricey ruthenium: The first catalyst systems using iron complexes for asymmetric H_2 hydrogenation at 50 °C and asymmetric transfer hydrogenation at room temperature has been discovered. The transfer hydrogenation activity is similar to that of the best ruthenium catalyst. Surprisingly, the precatalysts have a tetradentate diiminodiphosphine ligand which has no NH functionality.

Natural Products

K. C. Nicolaou,* D. Pappo, K. Y. Tsang,
R. Gibe, D. Y.-K. Chen* ———— **944 – 946**

A Chiral Pool Based Synthesis of Platensimycin

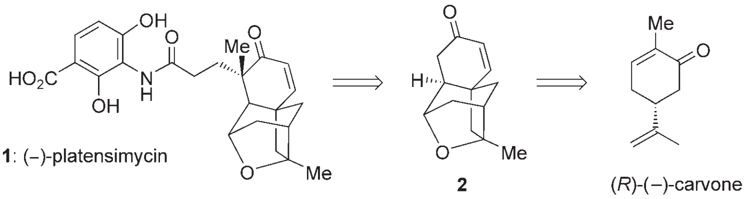

Extensive pharming: An expedient entry into the tetracycle **2**, a late-stage synthetic intermediate en route to the broad-spectrum antibiotic (−)-platensimycin (**1**) has been accomplished. The strategy involves a series of cyclizations starting from the inexpensive chiral pool starting material (*R*)-(−)-carvone.

Multicomponent Reactions

J.-M. Grassot, G. Masson,*
J. Zhu* ———— **947 – 950**

Synthesis of α-Ketoamides by a Molecular-Sieves-Promoted Formal Oxidative Coupling of Aliphatic Aldehydes with Isocyanides

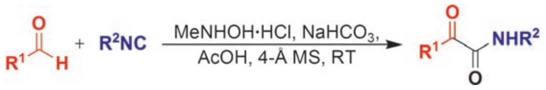

A twist in the Ugi four-component reaction: The reaction of an aldehyde, an isocyanide, *N*-methylhydroxylamine, and acetic acid in the presence of 4-Å molecular sieves afforded α-ketoamides in moderate to good yields (see scheme). In contrast, 3-Å molecular sieves did not promote the desired multicomponent reaction. R^1 = alkyl; R^2 = alkyl, aryl.

Metal-Catalyzed Cycloadditions

B. Trillo, F. López,* M. Gulías, L. Castedo,
J. L. Mascareñas* ———— **951 – 954**

Platinum-Catalyzed Intramolecular [4C+3C] Cycloaddition between Dienes and Allenes

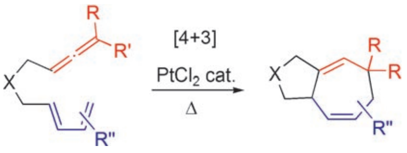

Crossing the seven C's: The three carbon atoms of several allenyl fragments can be incorporated into seven-membered carbocycles by means of a Pt-catalyzed intramolecular [4C+3C] cycloaddition with dienes (see scheme). The transformation provides a straightforward and atom-economical entry to a variety of cycloheptane-containing polycycles from readily available acyclic precursors.

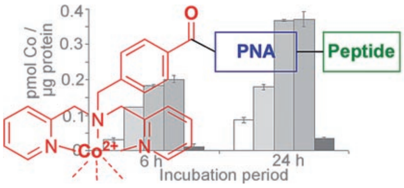

The metal does the trick! Atomic absorption spectroscopy (AAS) of cobalt atoms is used as an accurate method to determine the cellular uptake and nuclear localization of metal bioconjugates. Surprisingly, the PNA conjugates show highest uptake efficiency, and an accumulation 150% higher than in the culture medium is achieved.

Cellular Uptake

S. I. Kirin, I. Ott, R. Gust, W. Mier,
T. Weyhermüller,
N. Metzler-Nolte* ———— **955 – 959**

Cellular Uptake Quantification of Metalated Peptide and Peptide Nucleic Acid Bioconjugates by Atomic Absorption Spectroscopy

---

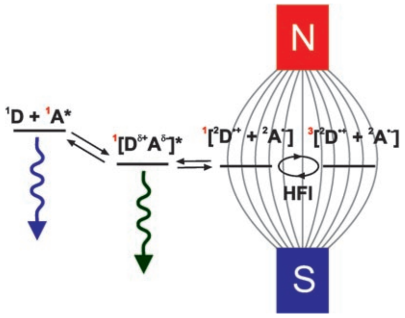

Separated and reunited: The photochemical magnetic field effect on the unbound fluorophore observed for 9,10-dimethylanthracene/*N*,*N*-dimethylaniline in mixtures of propylacetate/butyronitrile results from the radical pair mechanism in combination with extensive reversibility in the excited state (see picture; HFI: hyperfine interaction). This observation leads to a deeper understanding of the processes involving transient, spin-correlated radical ion pairs.

Fluorescence Systems

D. R. Kattnig, A. Rosspeintner,
G. Grampp* ———— **960 – 962**

Fully Reversible Interconversion between Locally Excited Fluorophore, Exciplex, and Radical Ion Pair Demonstrated by a New Magnetic Field Effect

---

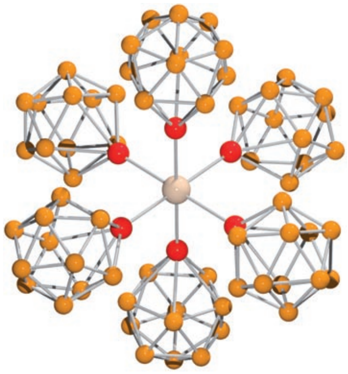

Aiming high: The coordination of the tin ligand stanna-*closo*-dodecaborate at Ni, Pd, and Pt results in the formation of compounds with high negative charges. These complexes contain metal centers with high coordination numbers and in high formal oxidation states. In the case of the platinum derivative, a far upfield chemical shift in the ^{195}Pt NMR spectrum ($\delta = -7724$ ppm) was observed.

Tin Coordination

VIP

M. Kirchmann, K. Eichele,
F. M. Schappacher, R. Pöttgen,
L. Wesemann* ———— **963 – 966**

Octahedral Coordination Compounds of the Ni, Pd, Pt Triad

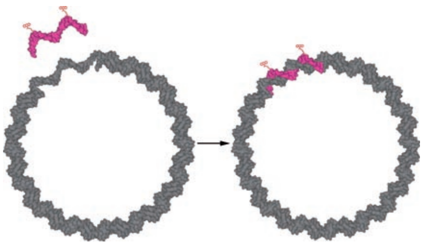

Doing the rounds: A highly straightforward approach has been developed that provides access to DNA minicircles containing a 21-mer single-stranded gap region of defined sequence (see picture). The single-stranded domain within a small circular DNA nanoobject provides the exciting opportunity to further functionalize a minicircle at defined positions in almost unlimited fashion, simply by hybridization with a synthetic 21-mer oligonucleotide.

DNA Structures (1)

G. Rasched, D. Ackermann, T. L. Schmidt,
P. Broekmann, A. Heckel,
M. Famulok* ———— **967 – 970**

DNA Minicircles with Gaps for Versatile Functionalization

DNA Structures (2)

G. Mayer, D. Ackermann, N. Kuhn, M. Famulok* ________ **971 – 973**

Construction of DNA Architectures with RNA Hairpins

Kissing complexes formed on the basis of highly specific noncanonical interactions of RNA hairpins can be harnessed for the controlled assembly of DNA nanoobjects. Two DNA minicircles, each equipped with a different RNA hairpin motif (see picture), mediate a tight and specific binding of the two circular DNA nanoobjects. These interactions may offer the possibility to construct DNA nanoobjects with increased complexity.

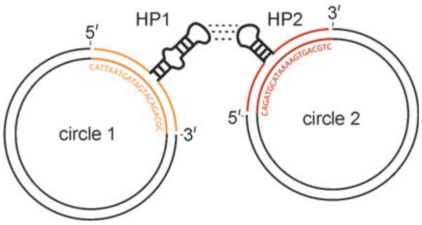

DNA Block Copolymers

F. E. Alemdaroglu, J. Wang, M. Börsch, R. Berger, A. Herrmann* ____ **974 – 976**

Enzymatic Control of the Size of DNA Block Copolymer Nanoparticles

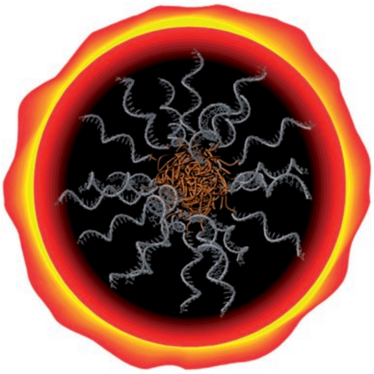

The right kind of upbringing: The size of DNA nanoparticles can be adjusted by an enzymatic reaction. By varying the incubation time of spherical nucleic acid block copolymer micelles (see picture) with a non-template-dependent DNA polymerase, the size of the nanoobjects can be gradually increased.

Protein Folding

S. Hiller, G. Wider, L. L. Imbach, K. Wüthrich* ________ **977 – 981**

Interactions with Hydrophobic Clusters in the Urea-Unfolded Membrane Protein OmpX

A denatured membrane protein in 8 M urea was characterized. Two hydrophobic clusters, separated by 50 amino acids in the polypeptide chain, are shown to bind independently to detergent micelles (see picture). Long-range interactions between the two clusters are not observed. These observations provide new insights into protein folding mechanisms.

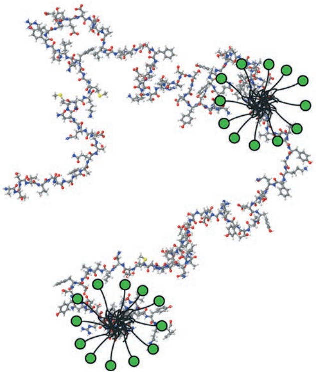

Supporting information is available on the WWW (see article for access details).

A video clip is available as Supporting Information on the WWW (see article for access details).

Service